Journal of Power Sources 254 (2014) 204–208

Contents lists available at ScienceDirect

Journal of Power Sources

journal homepage: www.elsevier.com/locate/jpowsour

Short communication

Transport properties of $LiCoPO_4$ and Fe-substituted $LiCoPO_4$

Jan L. Allen [a,*], Travis Thompson [b], Jeff Sakamoto [b], Collin R. Becker [a], T. Richard Jow [a], Jeff Wolfenstine [a]

[a] U.S. Army Research Laboratory, 2800 Powder Mill Road, Adelphi, MD 20783-1197, USA
[b] Michigan State University, Department of Chemical Engineering and Materials Science, East Lansing, MI 48824, USA

HIGHLIGHTS

- The ionic and electronic conductivities of dense, polycrystalline $LiCoPO_4$ and $Li_{1-x}Co_{0.9}Fe_{0.1}PO_4$ are measured and compared.
- $LiCoPO_4$ and $Li_{1-x}Co_{0.9}Fe_{0.1}PO_4$ are predominantly ionic conductors with relatively poor electronic conductivities.
- $Li_{1-x}Co_{0.9}Fe_{0.1}PO_4$ has higher bulk ionic and electronic conductivities than $LiCoPO_4$.

ARTICLE INFO

Article history:
Received 18 November 2013
Received in revised form
23 December 2013
Accepted 24 December 2013
Available online 4 January 2014

Keywords:
Li-ion
Battery
Cathode
Ionic
Electronic
Conductivity

ABSTRACT

$LiCoPO_4$ is a promising cathode material to enable high energy, abuse tolerant Li-ion batteries. However, $LiCoPO_4$ has relatively poor electronic conductivity which may be improved by chemical substitution. In this work, the ionic and electronic conductivities of dense, polycrystalline $LiCoPO_4$ and Fe^{2+}/Fe^{3+}-substituted $LiCoPO_4$ ($Li_{1-x}Co_{0.9}Fe_{0.1}PO_4$) are measured and compared. Both materials are predominantly ionic conductors with relatively good bulk ionic and relatively poor electronic conductivities. $Li_{1-x}Co_{0.9}Fe_{0.1}PO_4$ exhibits both higher bulk ionic and electronic conductivity. The increased bulk ionic conductivity of $Li_{1-x}Co_{0.9}Fe_{0.1}PO_4$ is believed to originate mainly from extra Li vacancies and the increased electronic conductivity is believed to originate mainly from creating more mobile hole polarons compared to $LiCoPO_4$ as a result of Fe^{2+}/Fe^{3+} substitution.

Published by Elsevier B.V.

1. Introduction

$LiCoPO_4$ is a potential high energy (~800 Wh kg^{-1}), abuse tolerant cathode material for use in Li-ion batteries [1] however, it suffers from capacity fade caused by structure deterioration and electrolyte decomposition [2–4]. Recent advances through Fe^{2+}/Fe^{3+}-substitution and electrolyte additives have now shown that the capacity fade can be significantly reduced [5] thereby increasing interest in this material. The substitution by Fe also significantly improves the rate capability of $LiCoPO_4$ as shown by electrochemical measurements on Fe^{2+}/Fe^{3+}-substituted $LiCoPO_4$ [5] or Fe^{2+}-substituted $LiCoPO_4$ [6,7]. Ruffo et al. [8] also report a significant enhancement in conductivity of Fe^{2+}-substituted $LiCoPO_4$ through transport measurements, however, the authors report that the significant enhancement in their samples most likely results from secondary phases such as carbon coming from the precursor or phosphides formed through carbothermal reduction. There are no prior reports on the transport properties of either carbon-free, Fe^{2+}-substituted $LiCoPO_4$ or on Fe^{2+}/Fe^{3+}-substituted $LiCoPO_4$ which is the subject of this paper. It is expected that Fe substitution will increase the intrinsic electronic conductivity of $LiCoPO_4$ as suggested by the combined experimental/computational paper of Johannes et al. [9] on the electronic structure of $LiMPO_4$ (M = Fe, Mn, Co and Ni) and its effect on the polaronic conductivity. The computations show that the energy for a polaron to move from one transition metal site to the next is lowest for $LiFePO_4$, therefore we believe that Fe^{2+} substitution into $LiCoPO_4$ will improve the electronic conductivity of $LiCoPO_4$. The ionic conductivity of $LiCoPO_4$ is also expected to improve in these samples owing to the presence of some Fe^{3+} (estimated to be ~60% Fe^{3+} via Mössbauer spectroscopy) on the Co or Li sites as described in detail by Allen et al. [5]. In order to maintain electro-neutrality, the Fe^{3+} on Li^+ or Co^{2+} sites is compensated by Li vacancies which should increase Li^+ ion mobility. In this paper, we will seek to understand the improvement

* Corresponding author. Tel.: +1 301 394 0291; fax: +1 301 394 0273.
E-mail addresses: jan.l.allen8.civ@mail.mil, jan_all@yahoo.com (J.L. Allen).

0378-7753/$ – see front matter Published by Elsevier B.V.
http://dx.doi.org/10.1016/j.jpowsour.2013.12.111

in rate capability of Fe^{2+}/Fe^{3+}-substituted $LiCoPO_4$ (hereafter referred to as $Li_{1-x}Co_{0.9}Fe_{0.1}PO_4$) compared to $LiCoPO_4$ through ionic and electronic transport measurements on hot-pressed samples of near theoretical density.

2. Experimental

$LiCoPO_4$ was prepared via a citrate complexation route [5]. $Co(OH)_2$ (Alfa Aesar), LiH_2PO_4 (Aldrich), and citric acid (Sigma–Aldrich), 1, 1.01, 1.02, molar ratio, respectively, were dissolved in deionized water. This solution was evaporated to dryness via a microwave oven. The resulting dried mass was ground lightly with mortar and pestle and heated in air at a rate of 10 K min^{-1} to 873 K and held at this temperature for 12 h. $Li_{1-x}Co_{0.9}Fe_{0.1}PO_4$ was prepared via nitrate co-precipitation [5]. $Li_{1-x}Co_{0.9}Fe_{0.1}PO_4$ was chosen based on the fact it had been shown to exhibit improved rate capability and cycling compared to $LiCoPO_4$ [5]. $Co(OH)_2$ (Alfa Aesar), LiH_2PO_4 (Aldrich) and $FeC_2O_4{\cdot}2H_2O$ (Aldrich), 0.9, 1.01,0.1 mol ratio, respectively were dissolved in 1 M HNO_3 (aq). The resulting nitrate solution was evaporated to dryness via a microwave oven in a fume hood and then heated under N_2 at a rate of 10 K min^{-1} to 873 K and held at this temperature for 12 h.

We chose hot-pressing as the consolidation method for samples in order to obtain highly dense samples. For most polycrystalline materials as the density increases the grain boundary resistance decreases thus making it in general easier to determine the bulk resistance [10–12]. Alternatively, one can choose to measure the conductivity of a single crystal in order to obtain the bulk conductivity. However, investigating polycrystalline material is more practical since actual Li-ion batteries employ polycrystalline material.

Dense discs of $LiCoPO_4$ and $Li_{1-x}Co_{0.9}Fe_{0.1}PO_4$ were prepared by hot-pressing of the powders at 1073 K at 62 MPa pressure for 0.5 h in graphite dies under Ar. Rectangular parallelepipeds were cut from the disc perpendicular to the pressing direction using a low-speed diamond saw and polished under mineral oil for density, micro-structural and electrical property measurements. The relative density values of the samples were determined by dividing the bulk density determined from the weight and volume by the theoretical density. Phase purity was evaluated using X-ray powder diffraction. Data were collected using a Rigaku Ultima III diffractometer (Cu Kα radiation).

Electrical conductivity measurements were performed on the hot-pressed $LiCoPO_4$ and $Li_{1-x}Co_{0.9}Fe_{0.1}PO_4$ samples using the two probe method. Pt was sputter coated on to the top and bottom surfaces of the specimens. Electrochemical impedance spectra (EIS), 0.1–10^6 Hz frequency range, 100 mV AC amplitude, 480–680 K temperature range and DC Polarization measurements, 2 V bias, 330–620 K temperature range were obtained using a Solartron 1260. The bulk, grain boundary and electrode contribution to the impedance were separated by fitting the spectra using ZView (Scribner Associates, Inc.). The DC polarization steady-state current and 2 V potential were used to determine the resistance which was converted to electronic conductivity using the specimen dimensions.

The microstructure of the hot-pressed $LiCoPO_4$ and $Li_{1-x}Co_{0.9}Fe_{0.1}PO_4$ samples was examined on fracture surfaces using scanning electron microscopy (FEI environmental SEM). The Fe distribution in $Li_{1-x}Co_{0.9}Fe_{0.1}PO_4$ was investigated in the SEM using energy dispersive X-ray spectroscopy (EDS) on fracture surfaces at an accelerating voltage of 20 kV.

3. Results and discussion

Fig. 1 shows the X-ray diffraction patterns of $LiCoPO_4$ (lower) and $Li_{1-x}Co_{0.9}Fe_{0.1}PO_4$ (upper) after hot-pressing. The patterns

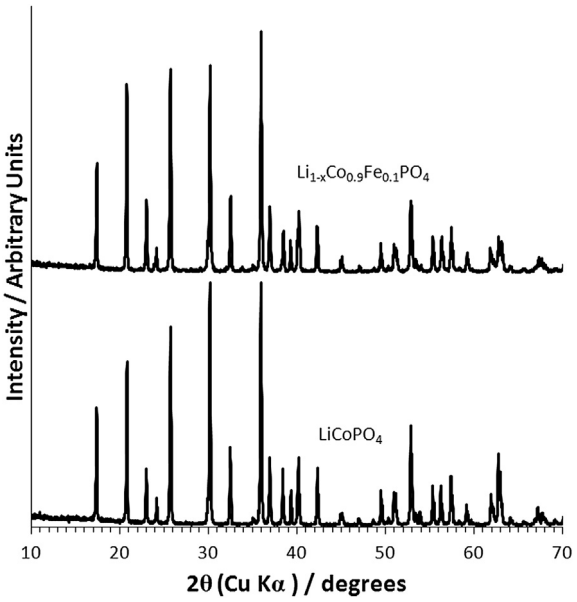

Fig. 1. XRD patterns of hot-pressed $LiCoPO_4$ (lower) and $Li_{1-x}Co_{0.9}Fe_{0.1}PO_4$ (upper).

confirm that a single phase was prepared in each case. Representative micrographs of the fracture surfaces of hot-pressed $LiCoPO_4$ and $Li_{1-x}Co_{0.9}Fe_{0.1}PO_4$ are shown in Figs. 2 and 3, respectively. From SEM analysis of $LiCoPO_4$ and $Li_{1-x}Co_{0.9}Fe_{0.1}PO_4$, a couple of points can be made. First, both samples are dense and very little porosity is observed in agreement with the relative density of ~98% determined from the physical dimensions, weight and the theoretical density calculated from the crystal structure. Second, no secondary phases were observed at the grain boundaries. Third, the grain sizes are approximately 4 and 10 microns for $LiCoPO_4$ and $LiCo_{0.9}Fe_{0.1}PO_4$, respectively. The difference in grain size suggests that Fe is affecting the materials diffusion during the synthesis. Additionally, since bulk conductivity is an important parameter for determining if a material will make a good Li-ion battery cathode, the difference in grain size highlights the importance to separate the grain boundary resistance from the bulk resistance during the data analysis. The grain size and density data are included in Table 1.

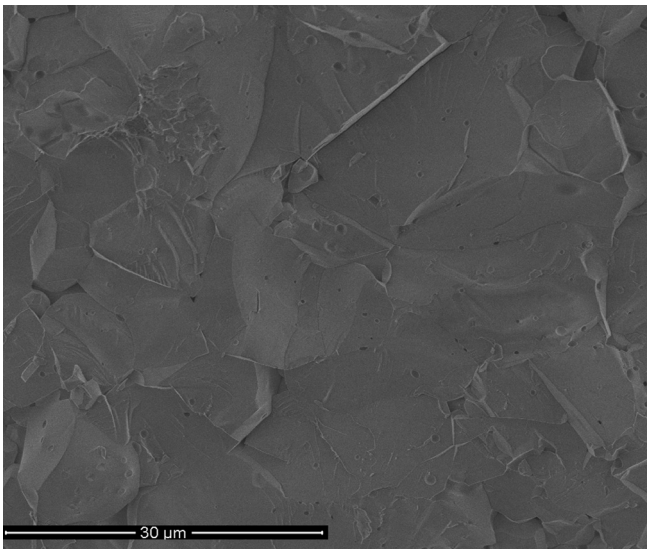

Fig. 2. Representative SEM image of a fracture surface of hot-pressed $LiCoFePO_4$.

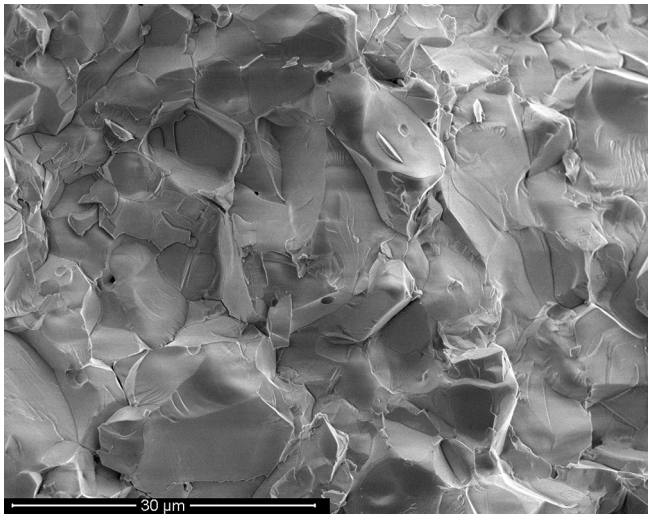

Fig. 3. Representative SEM image of a fracture surface of hot-pressed $Li_{1-x}Co_{0.9}Fe_{0.1}PO_4$.

Finally, preliminary EDS of $Li_{1-x}Co_{0.9}Fe_{0.1}PO_4$ confirmed X-ray diffraction measurements [5] that show that Fe is in the lattice and not segregated at grain boundaries. The EDS data is found in the Supplementary material.

Fig. 4 shows a representative impedance plot for $LiCoPO_4$ recorded at 678 K. For all samples of $LiCoPO_4$ and $Li_{1-x}Co_{0.9}Fe_{0.1}PO_4$ a similarly shaped spectrum was observed. We measured the EIS spectra in the temperature range 480–680 K because below 480 K the total ionic conductivity was below the minimum current limitations of our instrument. It should be noted that the impedance studies by Rissouli et al. [13] and Ruffo et al. [8] on $LiCoPO_4$ were also conducted over a nearly similar temperature range as that used in this study. The impedance spectra for all samples show a single semi-circle at higher frequency and a straight line at a slope of approximately 45° at lower frequency. Since we used Pt Li-ion blocking electrodes, the shape of the curve represents a material which is predominantly a Li^+ ion conductor with very low electronic conductivity [14,15]. The equivalent circuit used to model the impedance spectra is also shown on Fig. 4 and includes R_B, bulk or intra-grain impedance, R_{GB}, the grain boundary or inter-grain impedance, CPE_{GB}, the grain boundary constant phase element and $CPE_{electrode}$, the sample–electrode interface or dual layer constant phase element which is physically attributed to charge build-up at the Li-ion blocking Pt electrode.

Several points can be made from Fig. 4. First, the calculated value of the capacitance using the frequency at the maximum point of the semi-circle is shown on Fig. 4. This capacitance, $C = 3 \times 10^{-10}$ F, was calculated from $C_{GB} = (2\pi fR)^{-1}$, using $f = 1.36 \times 10^4$ Hz and R (diameter of the semi-circle) $= 4.51 \times 10^4\ \Omega$ [16]. This capacitance value is characteristic of a grain boundary [16] confirming our assignment of this semi-circle to a grain boundary phenomenon. Second, the value of the capacitance at the 45° sloping line is also calculated and shown on Fig. 4 using a typical point, $f = 0.40$ Hz, $Z'' = 1.56 \times 10^4\ \Omega$. The capacitance, $C = 2.6 \times 10^{-5}$ F, was calculated from $C_{DL} = (2\pi fZ'')^{-1}$ which is the

Table 1
Grain size, density and room-temperature-extrapolated transport properties of the $LiCoPO_4$ and $Li_{1-x}Co_{0.9}Fe_{0.1}PO_4$ compounds.

Composition	Grain size, microns	Density, g mL^{-1}	Relative density, %	$\sigma_{bulk\ Li\text{-}ion,\ 298\ K}$, S cm^{-1}	$\sigma_{elec,\ 298\ K}$, S cm^{-1}
$LiCoPO_4$	4	3.68	98	4×10^{-6}	8×10^{-16}
$Li_{1-x}Co_{0.9}Fe_{0.1}PO_4$	10	3.67	98	1×10^{-5}	2×10^{-12}

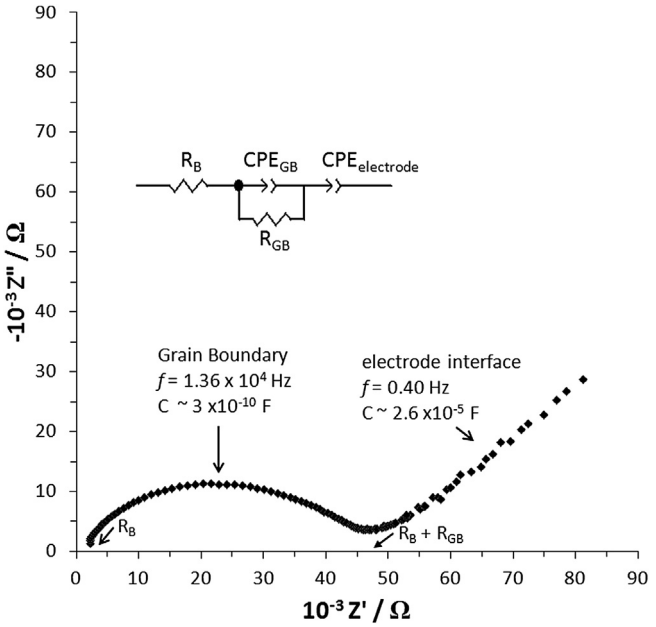

Fig. 4. Representative impedance plot of $LiCoPO_4$ recorded at 678 K and the equivalent circuit used to interpret the data.

equation applicable to a point on the line [16,17]. This capacitance value is characteristic of a capacitance that can be attributed to the sample–electrode interface [16] confirming our assignment to this phenomenon. With our interpretation validated, the bulk impedance value, R_B was taken from the Z' intercept at the high frequency of the semi-circle and the total impedance, $R_{total} = R_B + R_{GB}$, was taken from the Z' low frequency intercept. The values of R_B and R_{GB} and the physical dimensions of the sample were then used to determine the bulk and grain boundary Li-ion conductivity of $LiCoPO_4$ and $Li_{1-x}Co_{0.9}Fe_{0.1}PO_4$ as a function of temperature which were used to construct the Arrhenius plots (Fig. 5). The activation energy was estimated from the slope of the line in the temperature range 480–680 K.

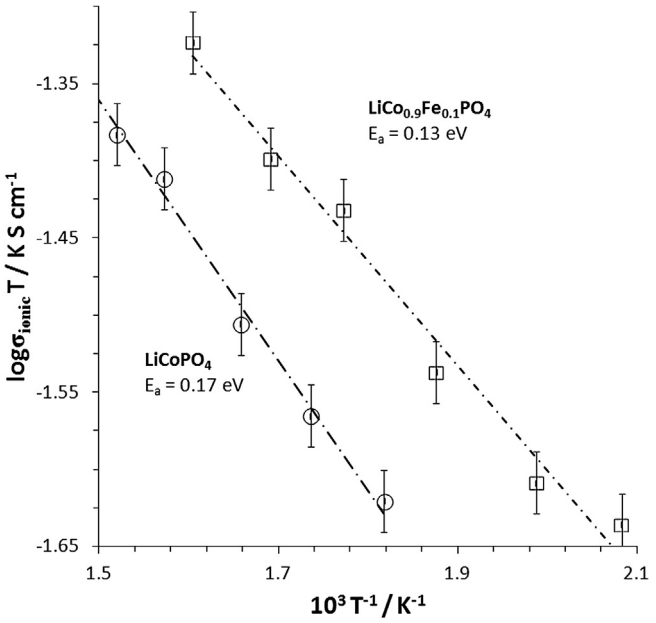

Fig. 5. Bulk ionic conductivity of $LiCoPO_4$ and $Li_{1-x}Co_{0.9}Fe_{0.1}PO_4$ as a function of temperature. Error bars represent the standard deviation.

From Fig. 5, several important points can be made. First, the bulk Li-ion conductivity of $Li_{1-x}Co_{0.9}Fe_{0.1}PO_4$ is higher at all temperatures. Second, the room temperature extrapolated values are 1×10^{-5} S cm^{-1} and 4×10^{-6} S cm^{-1} for $Li_{1-x}Co_{0.9}Fe_{0.1}PO_4$ and $LiCoPO_4$, respectively. This can be compared to the extrapolated room temperature ionic conductivity value for $LiCoPO_4$ of $\sim 10^{-8}$ S cm^{-1} and $\sim 10^{-14}$ S cm^{-1} from the reports of Ruffo et al. [8] and Rissouli et al. [13], respectively. Third, the activation energy for $Li_{1-x}Co_{0.9}Fe_{0.1}PO_4$ (0.13 eV) is slightly lower than that of $LiCoPO_4$ (0.17 eV). By comparison, Rissouli et al. [13] and Ruffo et al. [8] determined an activation energy value for $LiCoPO_4$ of 0.62 and 0.51 eV, respectively. In general, the reported conductivity values of Rissouli et al. [13] and Ruffo et al. [8] are lower, while the activation energy values are higher than those observed in this work and suggest that the authors' values are based on total ionic conductivity (bulk plus grain boundary) and not on bulk alone. For example, from the data of Rissouli et al. [13] it is not clear what intercept was used from their impedance to determine conductivity. Inspection of the impedance plot from Fig. 6 of Ruffo et al. [8] shows a frequency, f, at the semi-circle maximum of 10^5 Hz and a resistance of $\sim 1.1 \times 10^4$ Ω which per $C_{GB} = (2\pi fR)^{-1}$ gives a capacitance of $\sim 1.4 \times 10^{-10}$ F. This capacitance value suggests a significant grain boundary component [16]. Furthermore, we determined an activation energy of ~0.64 eV for the total ionic conductivity in $LiCoPO_4$, in rough agreement with above values, suggesting that the conductivity values and the activation energy determined by Rissouli et al. [13] and Ruffo et al. [8] most likely represent total conductivity and not bulk conductivity.

Prabu et al. [18] report a room temperature ionic conductivity value of 8.8×10^{-8} S cm^{-1} with activation energy of 0.43 eV for $LiCoPO_4$. Their impedance plots show a single semi-circle with a sloping line at low frequency similar to that shown in Fig. 4. However, they analyze the semi-circle based on a parallel combination of bulk resistance and bulk capacitance. An estimated capacitance value where data is available for the semi-circles gives a capacitance of about 4×10^{-11} F. This capacitance value suggests a grain boundary component [16]. Thus, explaining their lower conductivity and higher activation energy compared to the present results. In an earlier paper Prabu et al. [19] report a room temperature conductivity value of $\sim 1 \times 10^{-8}$ S cm^{-1} with activation energy of 0.48 eV for $LiCoPO_4$. However, if one determines the activation energy using their conductivity data from Table 1 of their paper [19] a value of 0.19 eV is obtained. This value is in good agreement with the activation energy determined in this study for bulk Li-ion conductivity in $LiCoPO_4$.

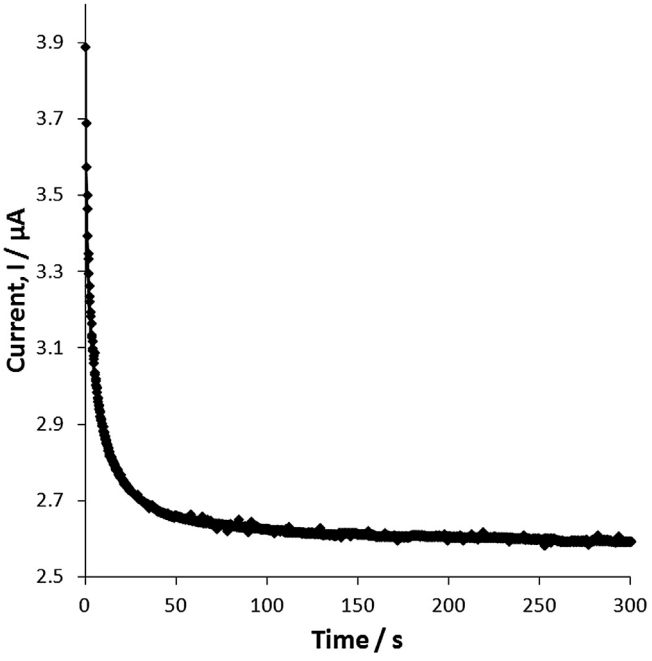

Fig. 6. Representative DC polarization curve of $LiCoPO_4$ at 619 K.

The extrapolated room temperature ionic conductivity for $LiCoPO_4$ can also be compared to a value of 9×10^{-4} S cm^{-1} [20] determined from the Nernst–Einstein equation using the Density Functional Theory (DFT) calculated diffusivity value reported by Morgan et al. [20]. The predicted value is ~225 times higher than the measured value in this study. The predicted value of Morgan et al. [20] can be considered to be the upper limit of ionic conductivity since it is calculated based on the ideal, defect-free $LiCoPO_4$ structure. In contrast, the $LiCoPO_4$ material used in this study contains anti-site defects (described below) which are known to reduce Li-ion mobility and subsequently lead to a lower ionic conductivity than in the ideal defect-free $LiCoPO_4$ [20,21]. Our activation energy (0.17 eV) for $LiCoPO_4$ is also lower than the DFT-predicted value of 0.36 eV for bulk Li diffusion reported by Morgan et al. [20]. Reasons for this difference are not apparent. It may be possible that as $LiCoPO_4$ becomes Li deficient, the activation energy decreases. Our $LiCoPO_4$ material most likely contains some non-stoichiometric defects (e.g., oxygen vacancies or Co^{3+}) leading to a Li deficient material. This suggestion is in agreement with the DFT calculations of Morgan et al. [20] who predict a value of the activation energy of 0.11 eV for low lithium content cobalt phosphate ($Li_{0.125}CoPO_4$). To confirm this suggestion, DFT calculations are needed at more Li values and a detailed characterization of the experimental $LiCoPO_4$ at various Li deficiencies is required.

In order to understand the higher bulk ionic conductivity of Fe-substituted $LiCoPO_4$, we briefly consider anti-site defects, lattice volume and the presence of Li^+ vacancies. First, we can rule out differences in the presence of anti-site defects such as Fe or Co on the Li site which would block Li-ion conduction in these 1-dimensional conductors and thereby lead to differences in the ionic conductivity. As shown by Allen et al. [5] through Rietveld analysis of X-ray diffraction data, the percent anti-site disorder on the Li site for $LiCoPO_4$ and $Li_{1-x}Co_{0.9}Fe_{0.1}PO_4$ are equal at $\sim 1.4 \pm 0.5\%$ for both samples. Thus, the difference in ionic conductivity does not result from a difference in the anti-site (Fe or Co on the Li site) concentration. On the other hand, the lattice volumes do vary between the two samples, 283.39(1) and 283.60(1) Å for $LiCoPO_4$ and $LiCo_{0.9}Fe_{0.1}PO_4$, respectively [5], consistent with the larger unit cell volume of $LiFePO_4$ relative to $LiCoPO_4$. The increased unit cell might enhance the mobility of the Li^+ ion. However, it is believed that the presence of some Fe^{3+} which creates Li^+ vacancies is most likely the predominant difference that results in higher bulk ionic conductivity for $Li_{1-x}Co_{0.9}Fe_{0.1}PO_4$ relative to un-substituted $LiCoPO_4$. The predictions of Morgan et al. [20] further support this viewpoint. The Li^+ ion diffusivity of $Li_{0.125}CoPO_4$, with almost 90% Li deficiency, was calculated to be 4 orders of magnitude higher than $LiCoPO_4$. In our case, we have only a few percent vacancies [5] so the effect on the ionic conductivity is much less.

To determine the electronic conductivity of $LiCoPO_4$ and $LiCo_{0.9}Fe_{0.1}PO_4$, DC polarization was undertaken. Fig. 6 is a typical example of the DC polarization behavior. It can be seen that there is a typical exponential decay of the current with measurement time. The electronic conductivity was estimated from the steady state current [22–24]. The measurements were done at elevated temperature owing to the low electronic conductivity of the sample and the current measurement limitation of our instrument. From the DC polarization measurement as a function of temperature and the physical dimensions of the samples, an Arrhenius plot of the electronic conductivities was constructed.

Fig. 7 shows the electronic conductivity of $LiCoPO_4$ and $Li_{1-x}Co_{0.9}Fe_{0.1}PO_4$ as a function of temperature. From Fig. 7, several important points can be made. First, the electronic conductivity of $Li_{1-x}Co_{0.9}Fe_{0.1}PO_4$ is higher than that for $LiCoPO_4$ at all measured temperatures. The room temperature electronic conductivities were found by extrapolation to be 8×10^{-16} and 2×10^{-12} S cm^{-1} for $LiCoPO_4$ and $LiCo_{0.9}Fe_{0.1}PO_4$, respectively. The introduction of Fe into $LiCoPO_4$ does increase the electronic conductivity 4 orders of magnitude, confirming predictions from DFT calculations [9]. The room temperature value for $LiCoPO_4$ can be compared to 9×10^{-11} S cm^{-1} reported by Tadanaga et al. [2]. Reasons for the difference between the two studies are not known. No details were given on how the DC conductivity was determined by Tadanaga et al. [2]. No values exist for electronic conductivity of $Li_{1-x}Co_{0.9}Fe_{0.1}PO_4$ at room temperature. The electronic conductivities of $LiCoPO_4$ and $Li_{1-x}Co_{0.9}Fe_{0.1}PO_4$ are 7–9 orders of magnitude lower than the bulk ionic conductivities. Thus, these materials are ionically conducting, electronically insulating materials. Secondly, the activation energies for electronic conductivity were found to be 0.97 and 0.58 eV for $LiCoPO_4$ and $LiCo_{0.9}Fe_{0.1}PO_4$, respectively. The lower activation energy for $Li_{1-x}Co_{0.9}Fe_{0.1}PO_4$ compared $LiCoPO_4$ is also in agreement with the DFT predictions [9]. Since, no activation energy values for electronic conductivity of $LiCoPO_4$ and $Li_{1-x}Co_{0.9}Fe_{0.1}PO_4$ have been published these can be best compared to the activation energy for electronic conduction in $LiFePO_4$ [25] where values range from 0.30 to 0.70 eV [25,26], 1.1 eV for $LiMnPO_4$ [26] and 0.53 eV for $LiFe_{0.45}Mn_{0.55}PO_4$ and $LiFe_{0.25}Mn_{0.75}PO_4$ [27]. The activation energy for electronic conductivity for $LiCoPO_4$ and $Li_{1-x}Co_{0.9}Fe_{0.1}PO_4$ is in agreement with other phospho-olivines where, the electronic conductivity is controlled by polarons [25–28]. Fortunately, the low electronic conductivity can be remedied by adding carbon through carbon additives or carbon coating the samples as has been used for the case of $LiFePO_4$ [26,29]. For example, Wolfenstine et al. [30] reported that the electronic conductivity of $LiCoPO_4$ could be increased from $<10^{-9}$ S cm^{-1} (below their instrumental limitation) to 10^{-4} to 10^{-5} S cm^{-1} by the addition of carbon.

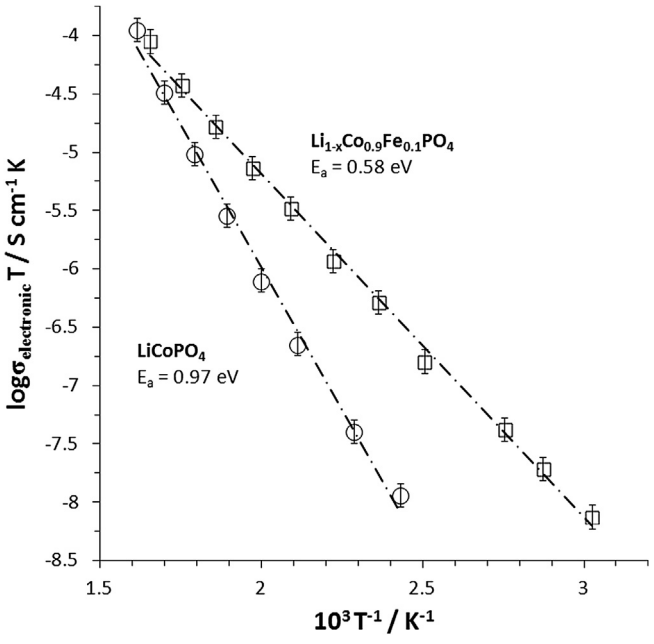

Fig. 7. Electronic conductivity of $LiCoPO_4$ and $Li_{1-x}Co_{0.9}Fe_{0.1}PO_4$ as a function of temperature. Error bars represent the standard deviation.

4. Conclusion

The ionic and electronic transport properties of $LiCoPO_4$ and $Li_{1-x}Co_{0.9}Fe_{0.1}PO_4$ Li-ion battery cathode materials were evaluated. Both materials are predominantly ionic conductors with relatively good bulk ionic conductivities of 4×10^{-6} and 1×10^{-5} S cm^{-1} and relatively poor electronic conductivities of 8×10^{-16} and 2×10^{-12} S cm^{-1}, for $LiCoPO_4$ and $Li_{1-x}Co_{0.9}Fe_{0.1}PO_4$ respectively. The introduction of Fe into the $LiCoPO_4$ structure improves both the electronic and bulk ionic conductivity compared to $LiCoPO_4$. Thus as expected, $Li_{1-x}Co_{0.9}Fe_{0.1}PO_4$ is a higher rate capable material compared to $LiCoPO_4$. The relatively good bulk ionic conductivity combined with an electronically conductive coating such as carbon makes $Li_{1-x}Co_{0.9}Fe_{0.1}PO_4$ a promising Li-ion battery cathode material owing to the expected high energy density and abuse tolerance.

Acknowledgments

JLA, CRB, TRJ and JW acknowledge support of the U.S. Army Research Laboratory (ARL).

Appendix A. Supplementary data

Supplementary data related to this article can be found at http://dx.doi.org/10.1016/j.jpowsour.2013.12.111.

References

[1] K. Amine, H. Yasuda, M. Yamachi, Electrochem. Solid-State Lett. 3 (2000) 178–179.
[2] K. Tadanaga, F. Mizuno, A. Hayashi, T. Minami, M. Tatsumisago, Electrochemistry 71 (2003) 1192–1195.
[3] N.N. Bramnik, K.G. Bramnik, T. Buhrmester, C. Baehtz, H. Ehrenberg, H. Fuess, J. Solid State Electrochem. 8 (2004) 558–564.
[4] J. Wolfenstine, U. Lee, B. Poese, J.L. Allen, J. Power Sources 144 (2005) 226–230.
[5] J.L. Allen, T.R. Jow, J. Wolfenstine, J. Power Sources 196 (2011) 8656–8661.
[6] D.W. Han, Y.M. Kang, R.Z. Yin, M.S. Song, H.S. Kwon, Electrochem. Commun. 11 (2009) 137–140.
[7] S.M.G. Yang, V. Aravindan, W.I. Cho, D.R. Chang, H.S. Kim, Y.S. Lee, J. Electrochem. Soc. 159 (2012) A1013–A1018.
[8] R. Ruffo, C.M. Mari, F. Morazzoni, F. Rosciano, R. Scotti, Ionics 13 (2007) 287–291.
[9] M.D. Johannes, K. Hoang, J.L. Allen, K. Gaskell, Phys. Rev. B 85 (2012) 115106.
[10] P.G. Bruce, A.R. West, J. Electrochem. Soc. 130 (1983) 662–669.
[11] R.D. Armstrong, T. Dickinson, P.M. Willis, J. Electroanal. Chem. 53 (1974) 389–405.
[12] J. Hu, J. Xie, X. Zhao, H. Yu, X. Zhou, G. Cao, J. Tu, J. Mater. Sci. Technol. 25 (2009) 405–409.
[13] K. Rissouli, K. Benkhouja, J.R. Ramos-Barrado, C. Julien, Mater. Sci. Eng. B 98 (2003) 185–189.
[14] R.A. Huggins, Ionics 8 (2002) 300–313.
[15] J.E. Bauerle, J. Phys. Chem. Solids 30 (1969) 2657–2670.
[16] J.T.S. Irvine, D.C. Sinclair, A.R. West, Adv. Mater. 2 (1990) 132–138.
[17] C.C. Hunter, M.D. Ingram, A.R. West, J. Mater. Sci. Lett. 1 (1982) 522–524.
[18] M. Prabu, S. Selvasekarapandian, M.V. Reddy, B.V.R. Chowdari, J. Solid State Electrochem. 16 (2012) 1833–1839.
[19] M. Prabu, S. Selvasekarapandian, A.R. Kulkarni, S. Karthikeyan, G. Hirankumar, C. Sanjeeviraja, Solid State Sci. 13 (2011) 1714–1718.
[20] D. Morgan, A. Van der Ven, G. Ceder, Electrochem. Solid-State Lett. 7 (2004) A30–A32.
[21] S.F. Yang, Y.N. Song, P.Y. Zavalij, M.S. Whittingham, Electrochem. Commun. 4 (2002) 239–244.
[22] M.A. Huang, T. Liu, Y.F. Deng, H.X. Geng, Y. Shen, Y.H. Lin, C.W. Nan, Solid State Ionics 204 (2011) 41–45.
[23] J.H. Kennedy, N. Kimura, S.M. Stuber, J. Electrochem. Soc. 129 (1982) 1968–1973.
[24] M. Hema, S. Selvasekarapandian, D. Arunkumar, A. Sakunthala, H. Nithya, J. Non-Cryst. Solids 355 (2009) 84–90.
[25] Y.-N. Xu, S.-Y. Chung, J.T. Bloking, Y.-M. Chiang, W.Y. Ching, Electrochem. Solid-State Lett. 7 (2004) A131–A134.
[26] A. Mauger, K. Zaghib, F. Gendron, C.M. Julien, Ionics 14 (2008) 209–214.
[27] C. Delacourt, L. Laffont, R. Bouchet, C. Wurm, J.-B. Leriche, M. Morcrette, J.-M. Tarascon, C. Masquelier, J. Electrochem. Soc. 152 (2005) A913–A921.
[28] J. Molenda, W. Ojczyk, J. Marzec, Solid State Ionics 177 (2006) 2617–2624.
[29] N. Ravet, Y. Chouinard, J.F. Magnan, S. Besner, M. Gauthier, J. Power Sources 97–98 (2001) 503–507.
[30] J. Wolfenstine, J. Read, J.L. Allen, J. Power Sources 163 (2007) 1070–1073.